J-11.2.3 Aquifer Sr-90 Simulation Results

The distribution of Sr-90 in the aquifer for the time period spanning 2005-2096 is given for the far-field in Figure J-11-22 with near-field results shown in Figure J-11-23 for the 2049-2151 time period. The resultant peak aquifer concentrations are given in Figure J-11-24. Because the Sr-90 originating in the vadose zone does not arrive in the aquifer until the mid 1980's, comparisons to measured data are not presented for aquifer wells.

Peak aquifer Sr-90 concentrations were predicted to be 5761 pCi/L in 1965 and are the result of the CPP-03 well. The simulated Sr-90 concentrations remained above the MCL from 1960 through year 2148. The Sr-90 concentrations in the aquifer are predicted to decline after the year 2000 with a step decrease in concentration following the removal of anthropogenic water at land surface in 2095. The predicted peak Sr-90 concentration in the year 2095 is 27.3 pCi/L, roughly 1.5 times higher than predicted for the base case (18.6 pCi/L).

Predicted aquifer concentrations for the year 2095 exceed the MCL by a factor of 3.4, with the majority of the long-term impact originating from the failed injection well. The Sr-90 contour plots presented in Figures J-11-22 and J-11-23 show the Sr-90 plume shrinking slowly in areal extent after the present time. Further, although Sr-90 concentrations in the aquifer are predicted to exceed the MCL through 2148, the area impacted by Sr-90 above 8 pCi/L is between the tank farm and the former percolation ponds by 2095, with a small area to the northeast of the tank farm. The extent is generally larger than predicted for the RI/BRA base case through the 2096 time period, but by 2151, the plumes are nearly identical.

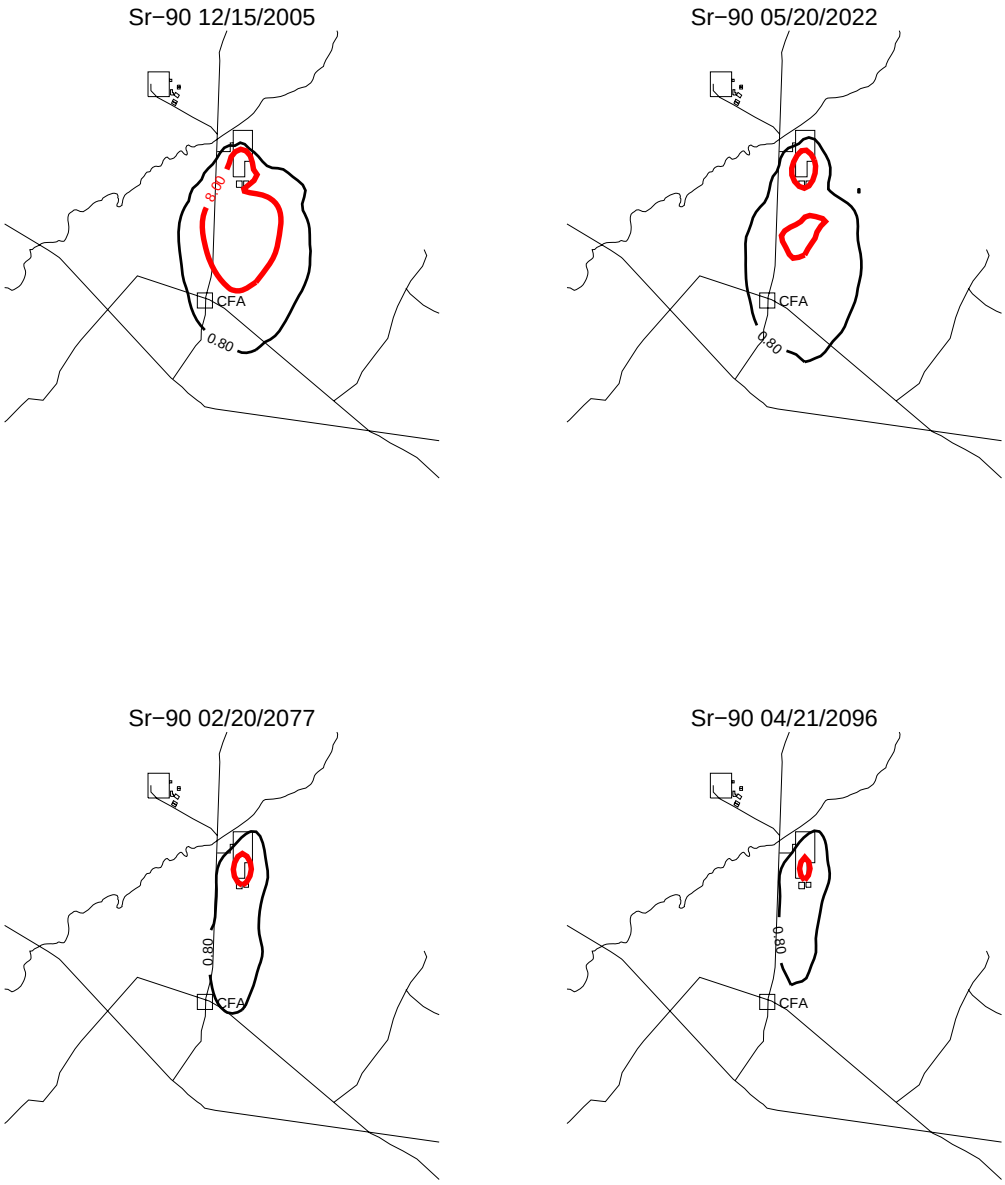

Figure J-11-22. Sr-90 aquifer concentration contours with higher 39 cm/yr infiltration through the tank farm (pCi/L) (MCL = thick red line, 10*MCL = thin red line, MCL/10 = black line).

Figure J-11-23. Sr-90 aquifer concentration contours with higher 39 cm/yr infiltration through the tank farm (pCi/L) (continued) (MCL = thick red line, 10*MCL = thin red line, MCL/10 = black line).

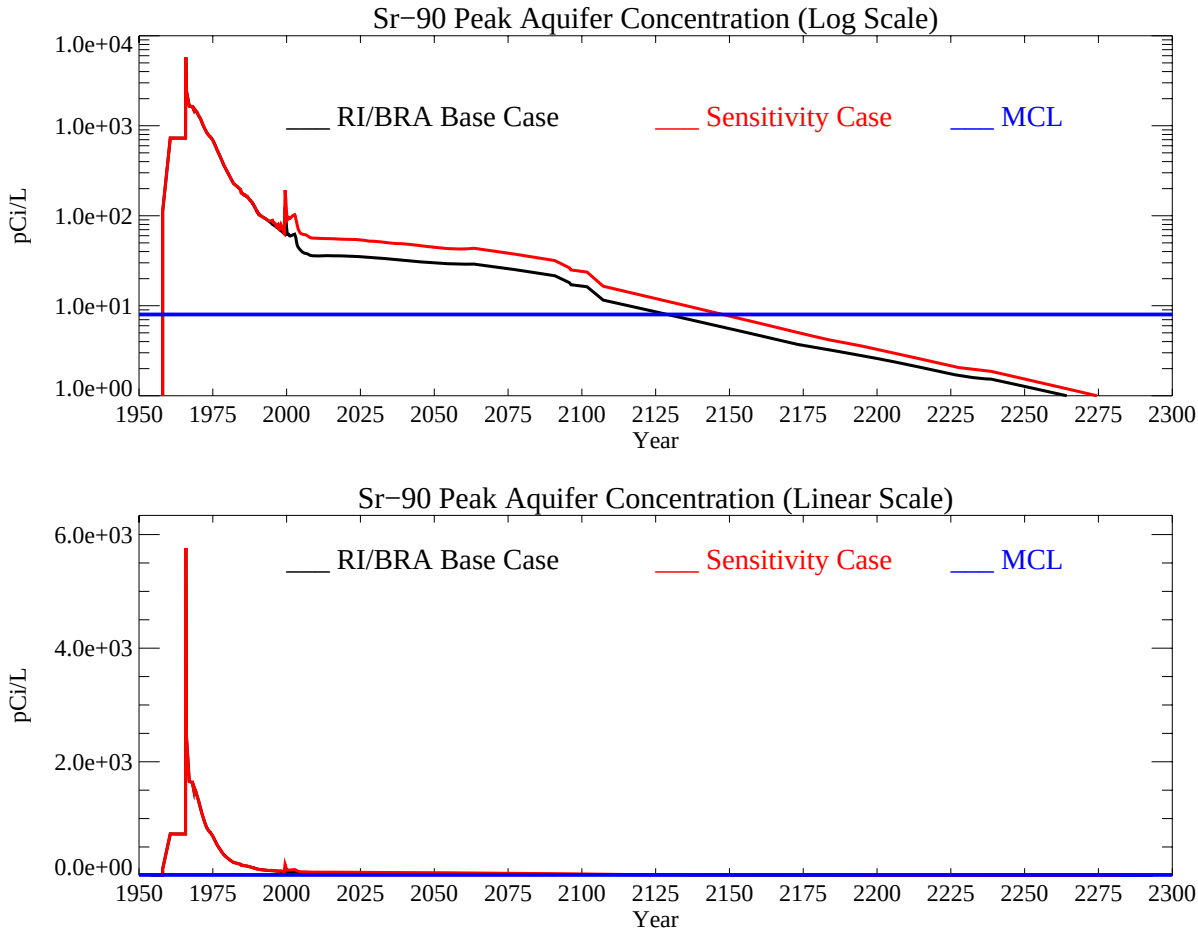

Figure J-11-24. Sr-90 peak aquifer concentrations with higher 39 cm/yr infiltration through the tank farm (pCi/L) with the MCL in blue, RI/BRA model in black and this sensitivity run in red.

J-11.3 Anthropogenic Water Focused in Northern INTEC

The sensitivity to higher anthropogenic recharge rates in northern INTEC was investigated by using a "worst case" infiltration scenario. The recharge rate used here was estimated from the imbalance between water production and known discharges to the percolation ponds. Recent records of the water production and final use at INTEC indicate that approximately 10 to 11 percent of the water produced is unaccounted for through existing metering. The total water usage in 2004 was approximately 495 million gallons and 10.5 percent of this volume is 52 million gallons. This volume of water represents metering inaccuracies, systems that are not metered (e.g., steam discharges, firewater testing, etc.), and other unintentional discharges. The density of utilities at the INTEC suggest that the discharge would be focused on the northern INTEC in an area of approximately 49 acres surrounding the tank farm.

In this infiltration scenario, the 52 million gallons were distributed across 49 acres, resulting in an anthropogenic recharge rate of 98 cm/year. This infiltration was in addition to the estimated recharge from precipitation of 18 cm/year, for a total of 116 cm/year. The simulated water was placed in the area surrounded by Palm Avenue, Hemlock street, Ash Avenue and the western INTEC security fence. The area beneath building 666 was also included. The area directly below the tank farm area was excluded from the higher water losses, and only 18 cm/year precipitation recharge was applied because most utilities do not run through the tank farm and the high and low tank farm infiltration sensitivity simulations assessed the sensitivity of tank farm contaminant mobility to recharge rate. The intent of this simulation was to investigate the movement of contaminants out of the perched water zones and to assess whether or not focusing the infiltration would result in complete saturation of the interbed regions. The high infiltration rate was applied for the entire assumed operational period of the INTEC (1954 through 2095). For comparison, the base case assumes that roughly 10 million gallons per year infiltrates over the entire developed INTEC facility (approximately 180 acres), equivalent to a rate of approximately 5 cm/year in addition to 18 cm/yr from precipitation.

Focusing this recharge outside of the tank farm allows the use of the activity-flux from the alluvium discussed in Section J-8.1, and therefore uses the RI/BRA flux of Sr-90 out of the alluvium.

J-11.3.1 Vadose Zone Sr-90 Simulation Results

The distribution of Sr-90 in the vadose zone is shown in Figures J-11-25 through J-11-28 through the year 2293. Compared to the RI/BRA base case, the horizontal extent of Sr-90 is further in the northern shallow vadose zone. This effect is more apparent in the comparison to field data presented in Figure J-11-29.

The predicted Sr-90 concentrations in perched water wells (Figures J-11-29 and J-11-30) show that observed concentrations in shallow well completions (MW-33-1 and MW-55-06) are better matched with these increased fluxes. This better match occurs because the higher fluxes push Sr-90 out laterally from directly beneath the tank farm through the upper portion of the shallow northern perched water. Concentrations in wells closer to the tank farm (MW-10-2 and MW-20-2) are over predicted because too much Sr-90 is being driven downward. In wells an intermediate distance from the tank farm, there is an overall slight decrease in perched water concentrations because of dilution in the upper shallow interbed. In addition, there is increased lateral movement toward wells MW-02, 55-06, 4-2, and 18-1. The wells near the former percolation ponds are not as affected because the percolation pond discharges are much higher than discharges in the RI/BRA model from other anthropogenic waters.

Peak vadose zone concentrations for this simulation are represented by the red line in Figure J-11-31 and are somewhat lower at late times relative to the RI/BRA base case shown in black. Highest concentrations 4.0E8 pCi/L) in the vadose zone are predicted to occur in 1978 as activity released during the first 20 years after the CPP-31 release combine with those from CPP-79 in the vadose zone.

The rate at which this activity enters the aquifer is given in Figure J-11-32 by the red line, and can be compared directly to the RI/BRA base case shown in black. The large difference in anthropogenic water results in a significant increase in flux leaving the vadose zone throughout the entire simulation period. In both cases, the anthropogenic water is removed in year 2095.

Figure J-11-25. Sr-90 vadose zone concentration with anthropogenic water focused in northern INTEC (horizontal contours) (pCi/L) (MCL = thick red line, 10*MCL = thin red line, MCL/10 = black line).

Figure J-11-26. Sr-90 vadose zone concentration with anthropogenic water focused in northern INTEC (horizontal contours) (pCi/L) (MCL = thick red line, 10*MCL = thin red line, MCL/10 = black line).

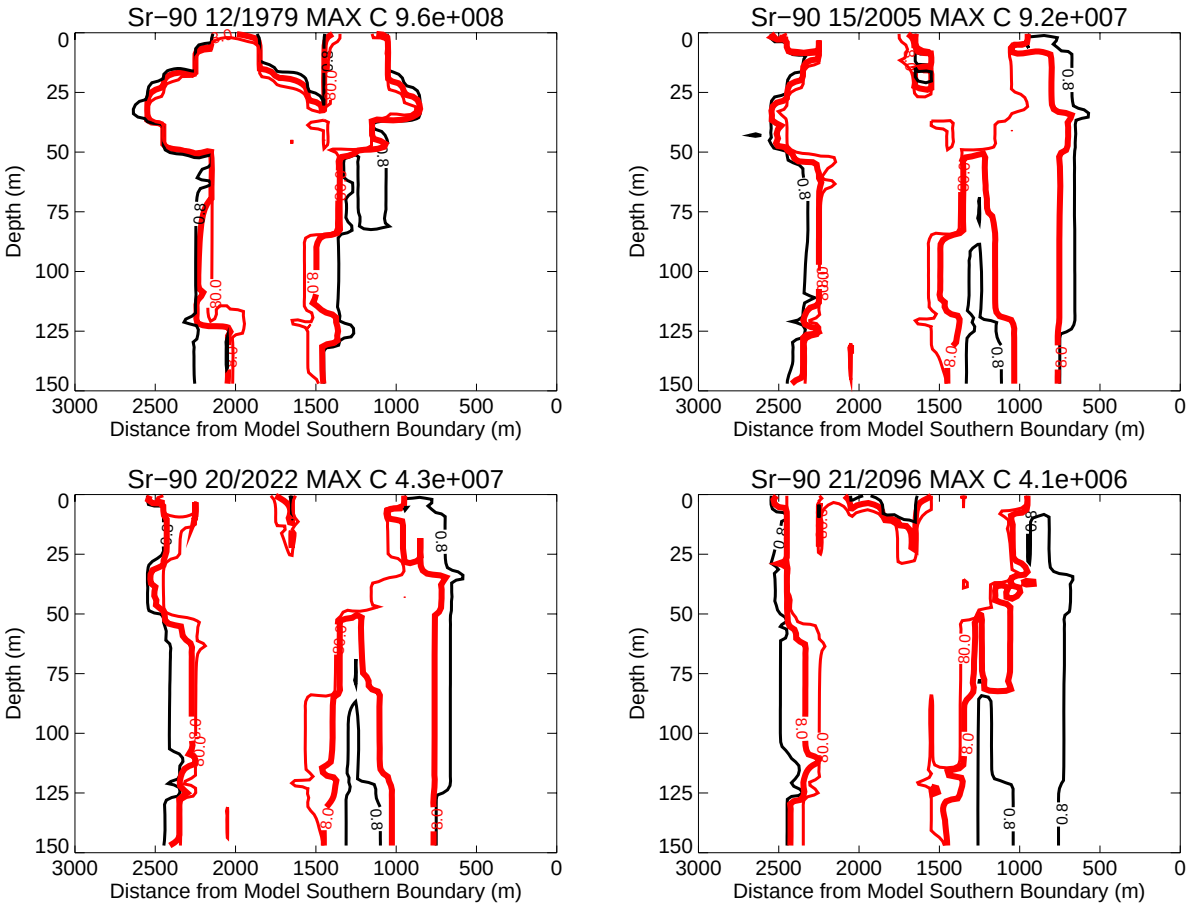

Figure J-11-27. Sr-90 vadose zone concentrations with anthropogenic water focused in northern INTEC (vertical contours) (pCi/L) (MCL = thick red line, 10*MCL = thin red line, MCL/10 = black line).

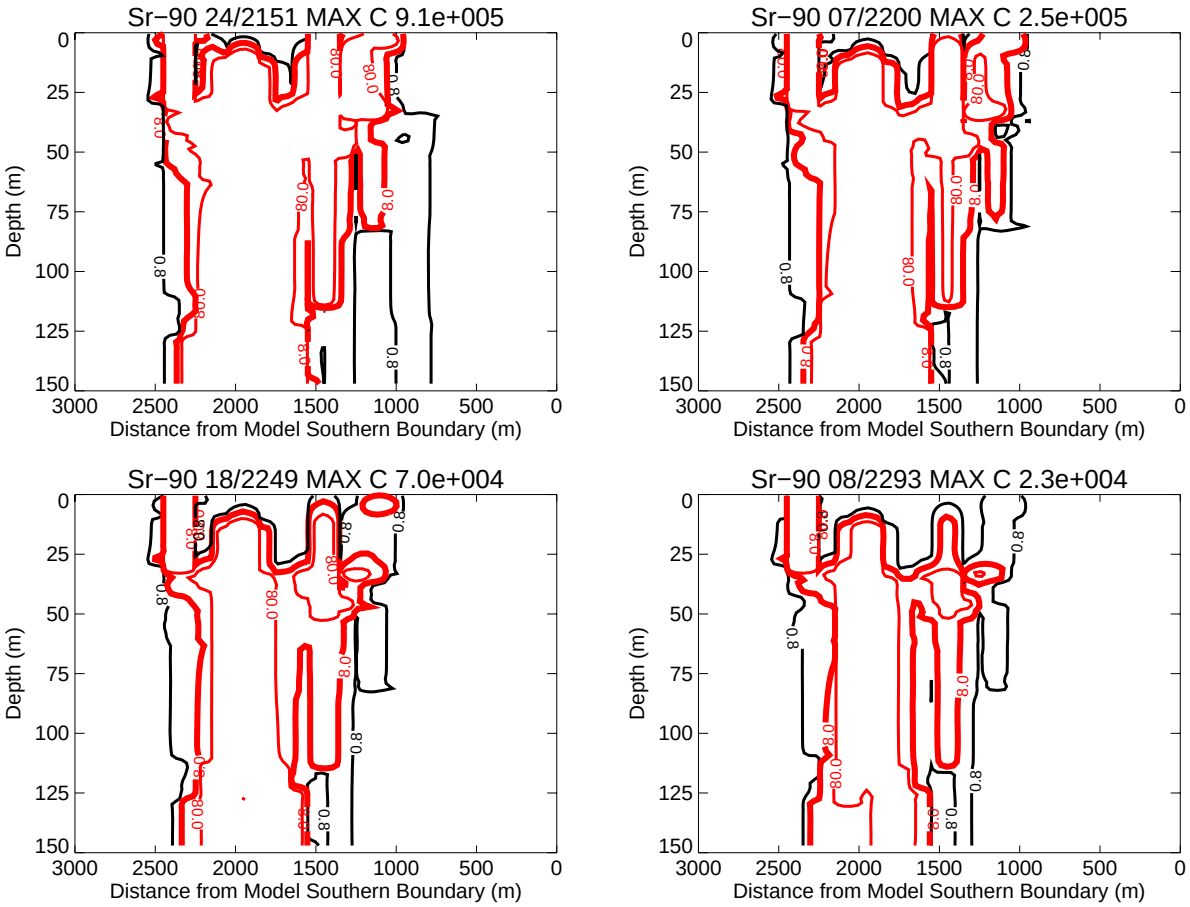

Figure J-11-28. Sr-90 vadose zone concentrations with anthropogenic water focused in northern INTEC (vertical contours) (pCi/L) (continued) (MCL = thick red line, 10*MCL = thin red line, MCL/10 = black line).

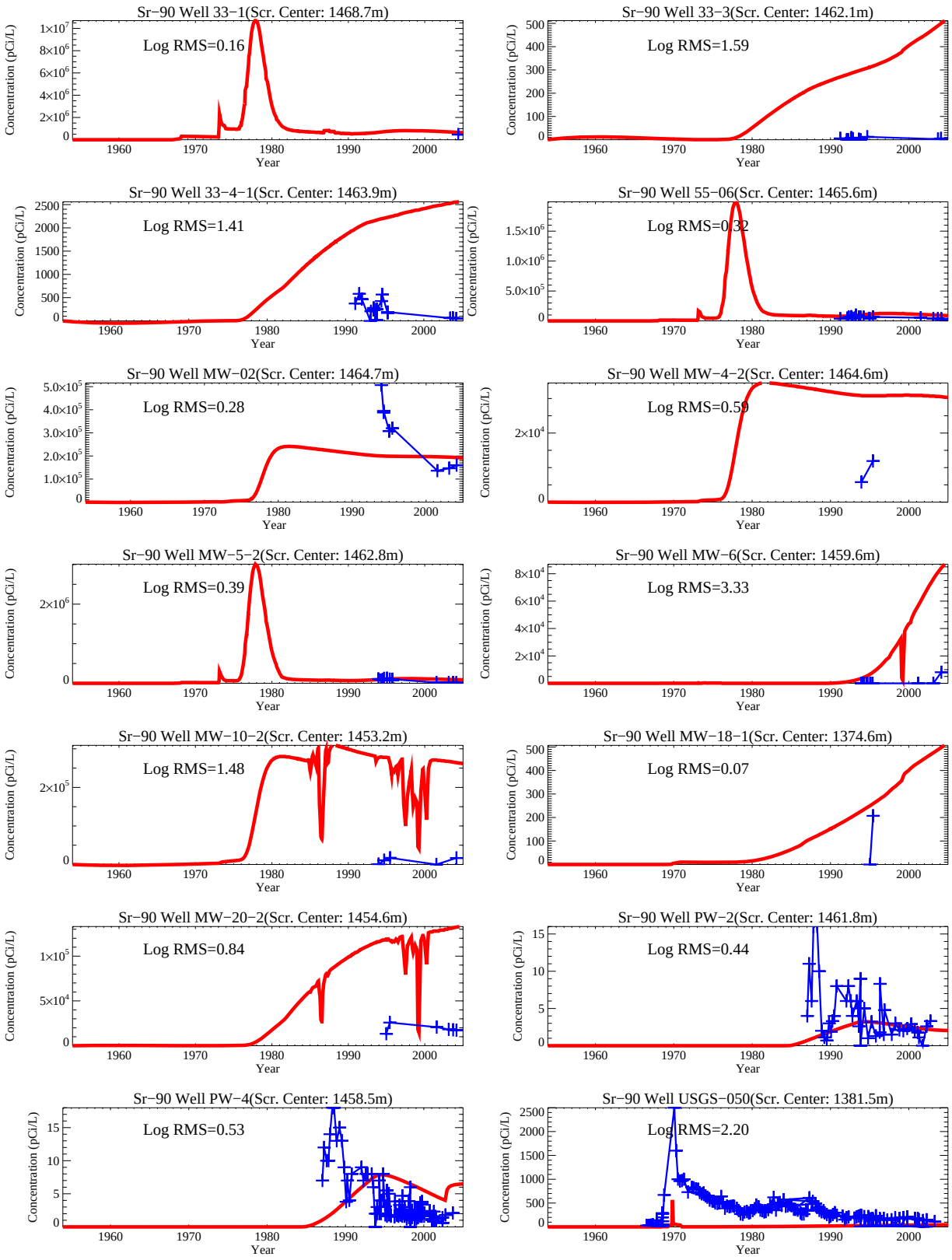

Figure J-11-29. Sr-90 concentration in perched water wells with anthropogenic water focused in northern INTEC (pCi/L) (Measured values = blue crosses, red = model at screen center).

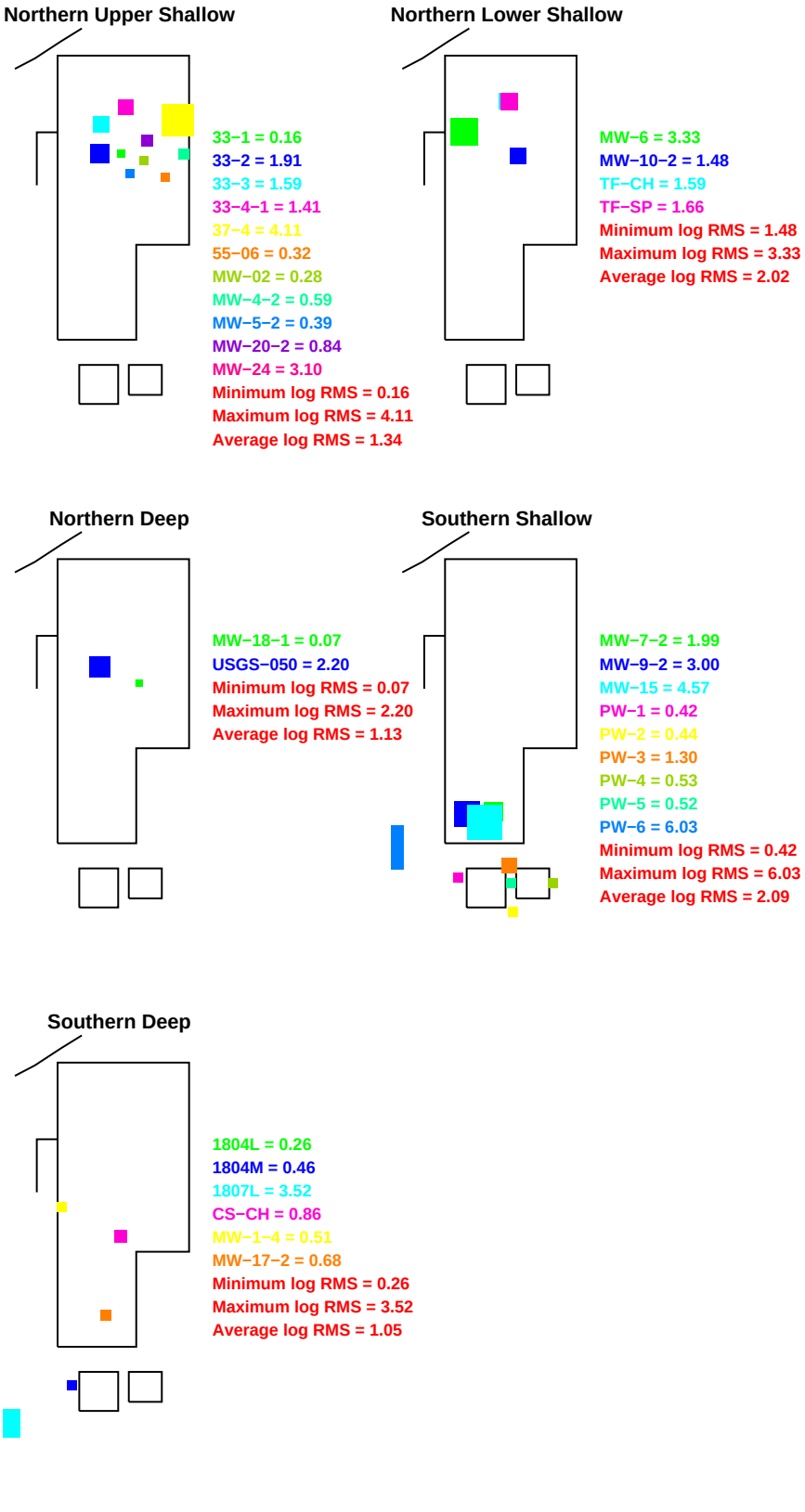

Figure J-11-30. Log 10 Root mean square error (RMS) by depth and northing with anthropogenic water focused in northern INTEC.

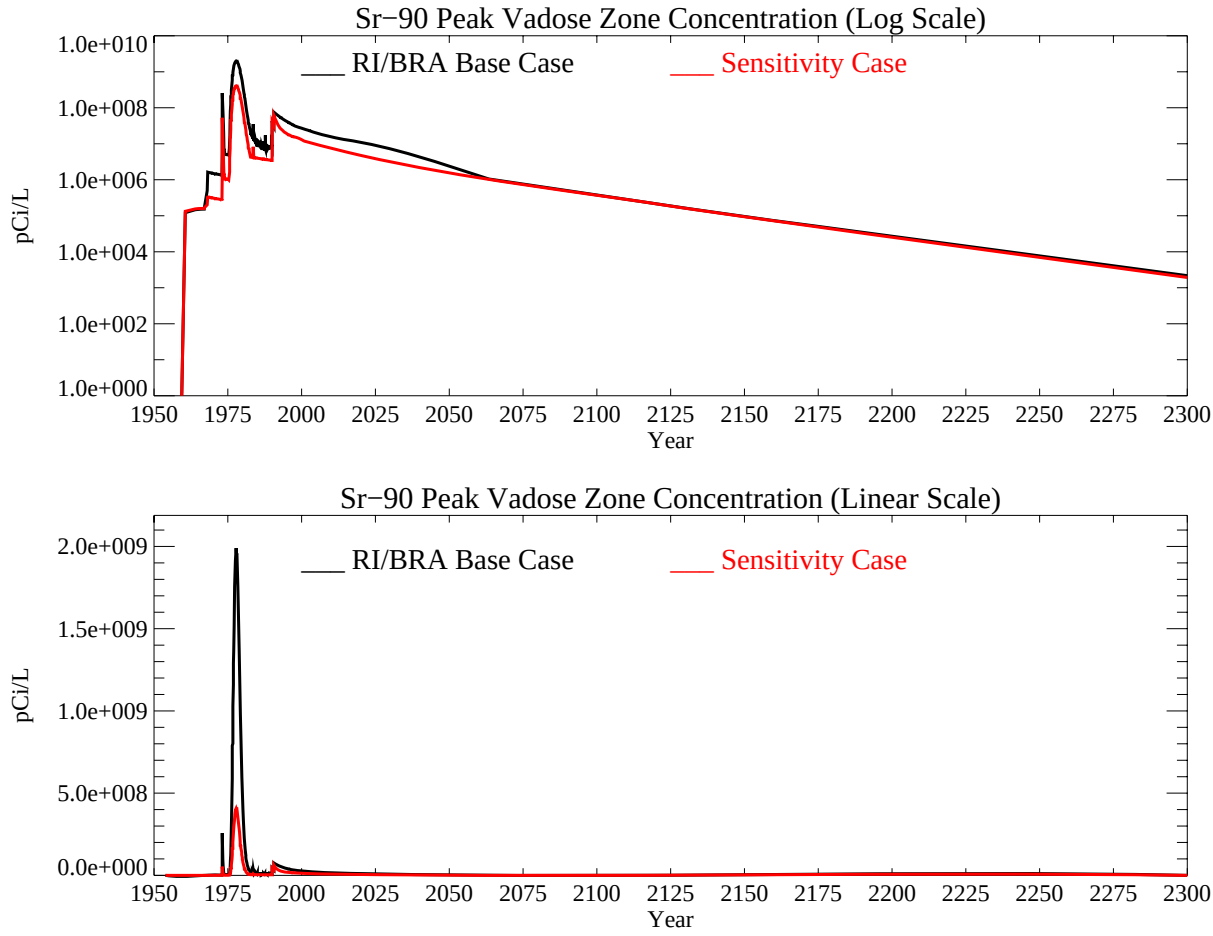

Figure J-11-31. Sr-90 peak vadose zone concentrations with anthropogenic water focused in northern INTEC (pCi/L). The RI/BRA model is shown in black and this sensitivity run in red.

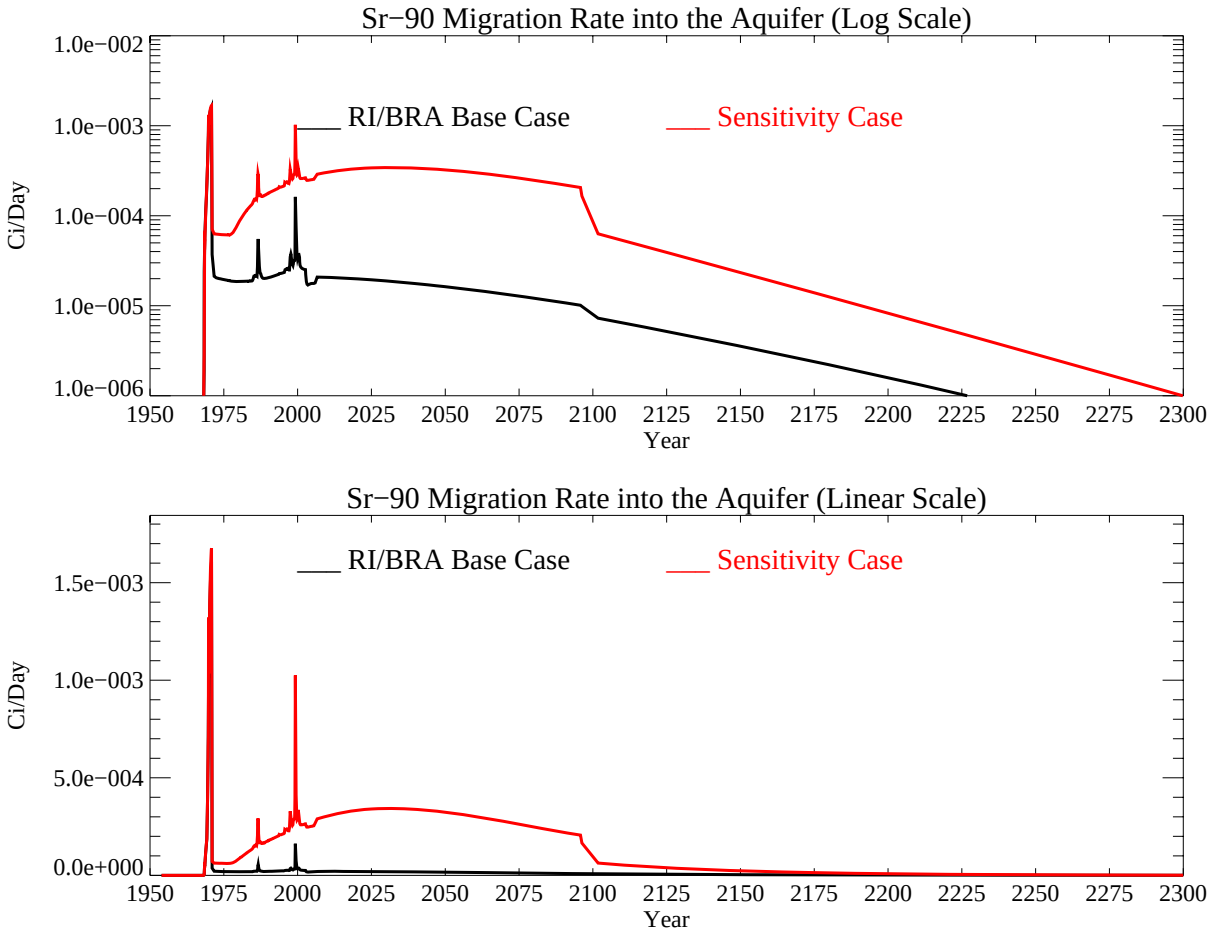

Figure J-11-32. Sr-90 activity flux into the aquifer (Ci/day) with anthropogenic water focused in northern INTEC. The RI/BRA model is shown in black and this sensitivity run in red.

J-11.3.2 Aquifer Sr-90 Simulation Results

The distribution Sr-90 in the aquifer for the time period spanning 2005-2096 is shown for the far field in Figure J-11-33 and in the near field in Figure J-11-34 for the 2049-2151 time period. The resultant peak aquifer concentrations are given in Figure J-11-35. Based on these results, in year 2095, the predicted peak concentration is 343 pCi/L, 18.5 times higher than predicted in the RI/BRA base case. This is much higher than predicted in the other simulations because the higher infiltration rate decreases the residence time in the vadose zone. As a result, Sr-90 is not allowed to decay while still in the vadose zone. Increasing the anthropogenic water in northern INTEC keeps simulated Sr-90 concentrations above the MCL from 1960 through year 2214. Further, the Sr-90 concentrations in the aquifer are not predicted to decline until after the year 2020. Compared to the RI/BRA base case, this is an additional 85 years during which remedial actions must be successful.

Available Sr-90 data in the aquifer does not support this infiltration rate. Measured data from the SRPA indicates that Sr-90 concentrations are currently declining in the aquifer with current values less than 40 pCi/L. With this infiltration rate, the peak concentration for year 2005 is approximately 672 pCi/L, 17 times higher than the observed data. Further, the predicted concentrations do not decline significantly until at least 2020. Higher flux rates from the alluvium are not attenuated naturally by aquifer water passing beneath the

tank farm, and this keeps the areal extent of Sr-90 above the MCL from shrinking. In all of the other sensitivity results obtained in this study, the Sr-90 plume was predicted be reduced in size after the present time which is consistent with measured data. All of other simulations show that there should be a significant reduction in plume size by 2010. If this scenario is correct, Sr-90 concentrations should just now be decreasing in the aquifer.

Calibration to Sr-90 data was performed separately in the vadose zone and in the aquifer. If observed data in the northern upper shallow perched water (100 ft) were used independently of the other perched water or aquifer results, it would suggest that more anthropogenic water is being discharged in northern INTEC than assumed in the RI/BRA base case. However, the match to field data in the northern lower upper shallow perched water (140 ft) and the match to aquifer data indicates that the infiltration rates here are too high. Because of this apparent discrepancy, it is important to recognize why the average RMS is lower in perched water wells in the northern upper shallow perched water in this case.

Standing free perched water above the 110 ft and 140 ft interbeds directly under the tank farm is not created using the base flux rates for any of the model simulations. As a result, lateral advection and dispersion in the model is forced to occur through the interbeds. While traveling through the interbeds, the transported Sr-90 is subjected to adsorption which lowers the concentrations and retards lateral movement. Increasing the flux rates allows more advection to occur high in the interbed and just below the basalt-interbed contact. The lateral migration of Sr-90 in this simulation accounts for the better match to field data for wells in the 110 ft interbed. However, this high infiltration rate also drives more Sr-90 deeper into the 140 ft interbed, resulting in overpredicting observed concentrations in the northern lower shallow perched water and a worse match to field data.

Simultaneously matching observed aquifer concentrations, concentrations in the 140 ft interbed, and the higher concentrations to the southeast of the tank farm in the northern upper shallow perched water might be accomplished by lowering the permeability of the 110 ft interbed and using a slightly higher K_d.

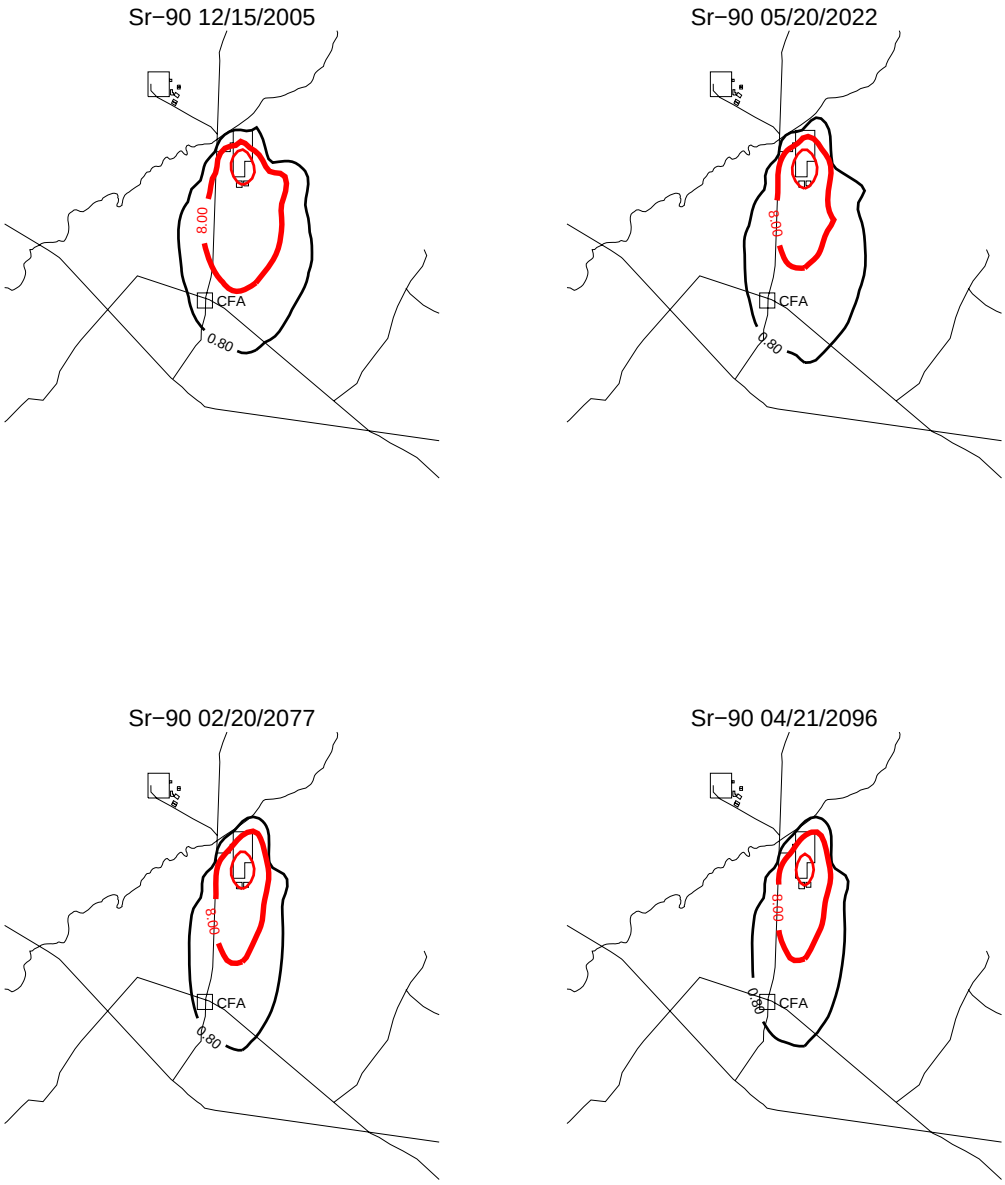

Figure J-11-33. Aquifer concentration contours with anthropogenic water focused in northern INTEC (pCi/L) (MCL = thick red line, 10*MCL = thin red line, MCL/10 = black line).

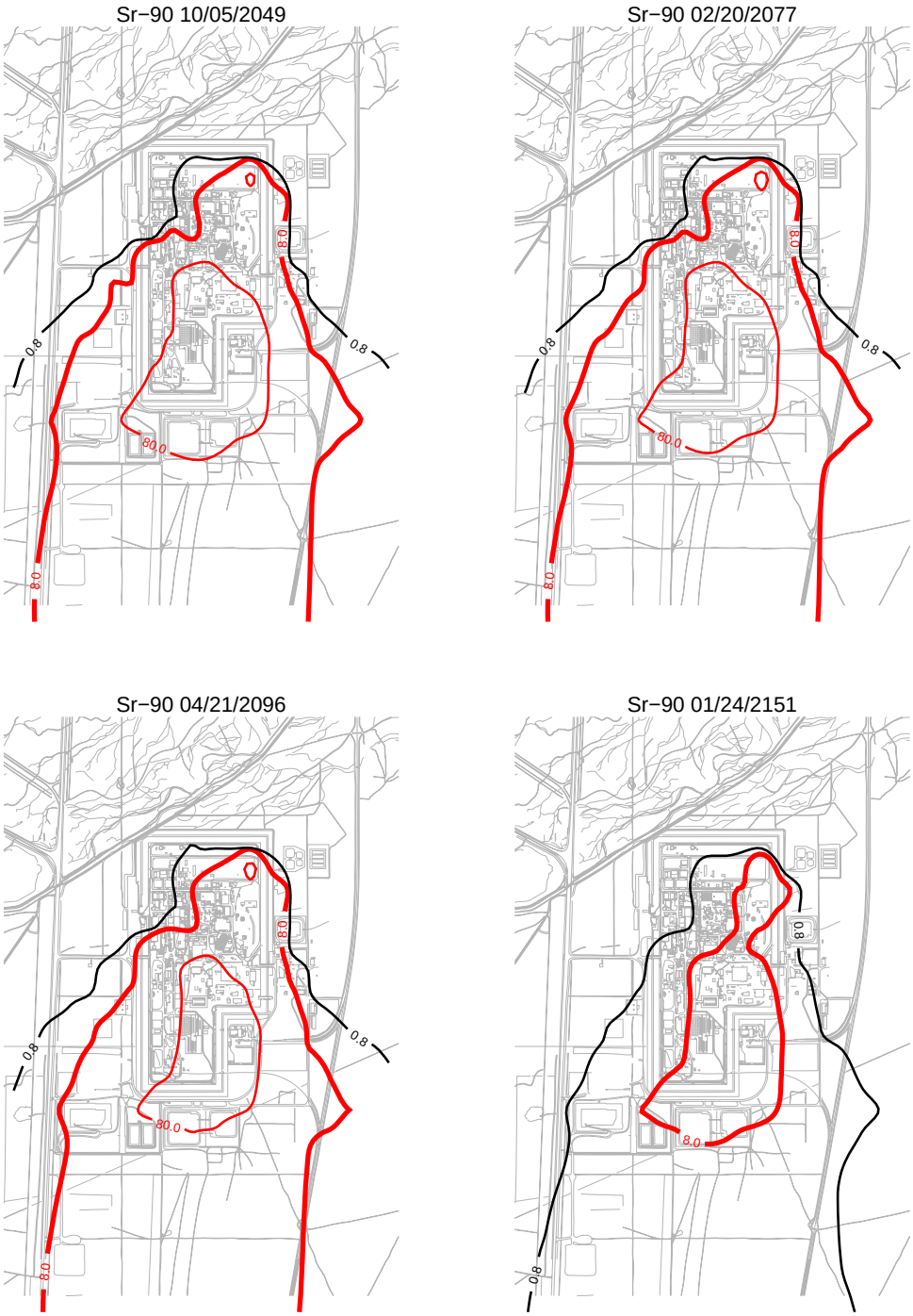

Figure J-11-34. Sr-90 aquifer concentration contours with anthropogenic water focused in northern INTEC (pCi/L) (continued) (MCL = thick red line, 10*MCL = thin red line, MCL/10 = black line).

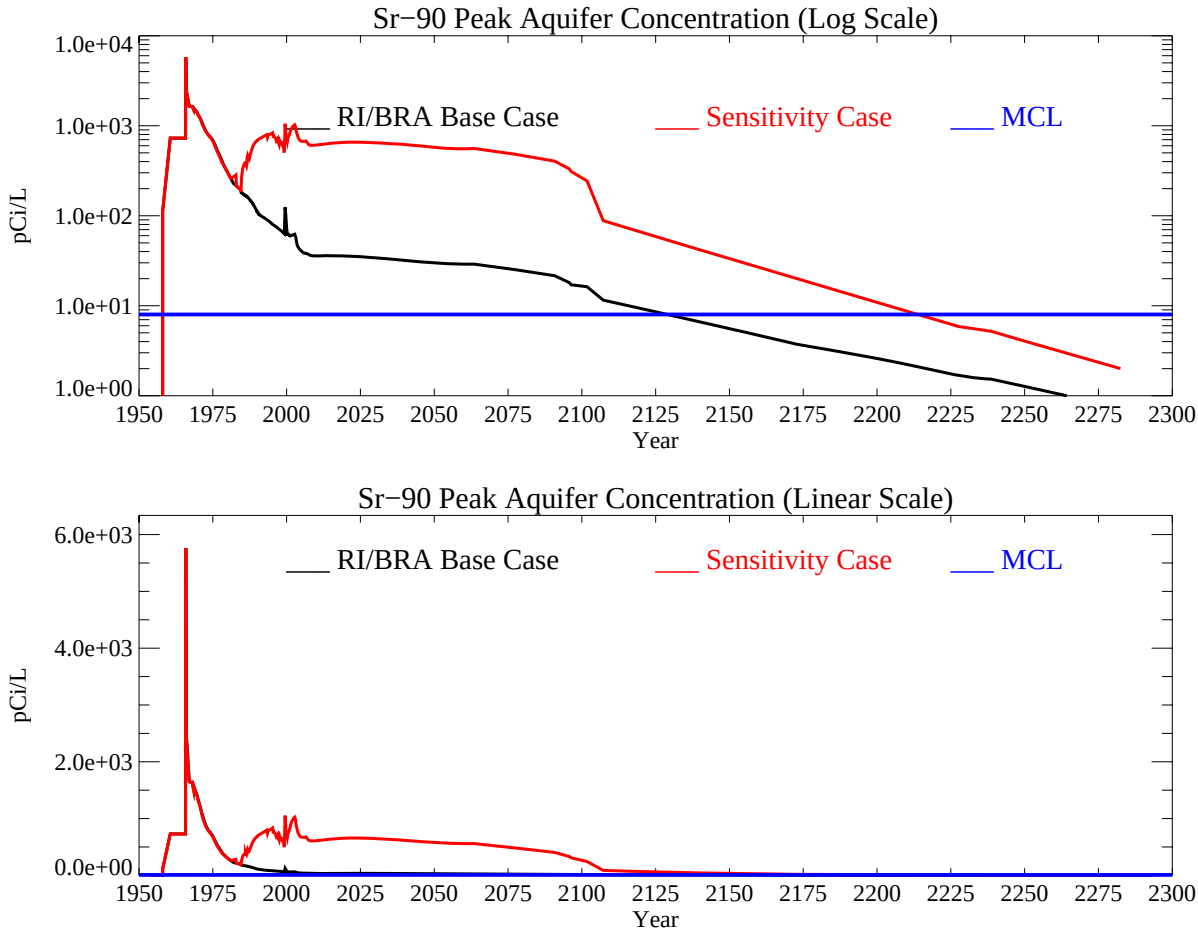

Figure J-11-35. Sr-90 peak aquifer concentrations with anthropogenic water focused in northern INTEC (pCi/L) with the MCL in blue, RI/BRA model in black and this sensitivity run in red.

J-11.4 Stopping Anthropogenic Water Losses In Year 2035

Each of these sensitivity simulations has suggested that anthropogenic water contributes to the downward movement of Sr-90 from the perched water regions. This has been apparent in the step-decrease in activity leaving the vadose zone and the corresponding decrease in aquifer concentrations following the removal of anthropogenic water in 2095. INTEC operations is in the process of reducing their anthropogenic water losses through a series of activities. If these activities are successful, or if operations at INTEC are significantly reduced, there will be a commensurate decrease in anthropogenic water losses to the vadose zone. This sensitivity analysis examines the impact on the transport of Sr-90 assuming anthropogenic water losses cease in year 2035, as opposed to continuing through year 2095 as assumed in the RI/BRA base case.

J-11.4.1 Vadose Zone Sr-90 Simulation Results

This simulation uses the activity-flux from the alluvium corresponding to the RI/BRA base case discussed in Section J-8. Figures J-11-36 through J-11-39 illustrate the horizontal and vertical distribution of the Sr-90 in the vadose zone through the year 2293. Figure J-11-40 illustrates Sr-90 arrival in key perched water wells, and the comparison to field data for all perched water wells is shown in Figure J-11-41. The first 3 subplots in Figure J-11-36 are identical to the base case as are the comparisons to field data because the anthropogenic water was not removed until 2035. The later-time subplots presented in Figure J-11-39 are also not significantly different than those presented for the RI/BRA base case.

Predicted peak vadose zone concentrations through time are given in Figure J-11-42 and are not significantly different than those presented for the base case. The highest concentration is 2.0E9 pCi/L which is equal to that obtained in the base case. The rate at which this activity enters the aquifer is given in Figure J-11-43, and can be compared directly to the base case (shown as black). Note that decreasing anthropogenic water in year 2035 relative to decreasing it in year 2095 results in a modest change in flux rates out of the aquifer only during the 2035-2095 time period.

Figure J-11-36. Sr-90 vadose zone concentration stopping anthropogenic water losses in 2035 (horizontal contours) (pCi/L) (MCL = thick red line, 10*MCL = thin red line, MCL/10 = black line).

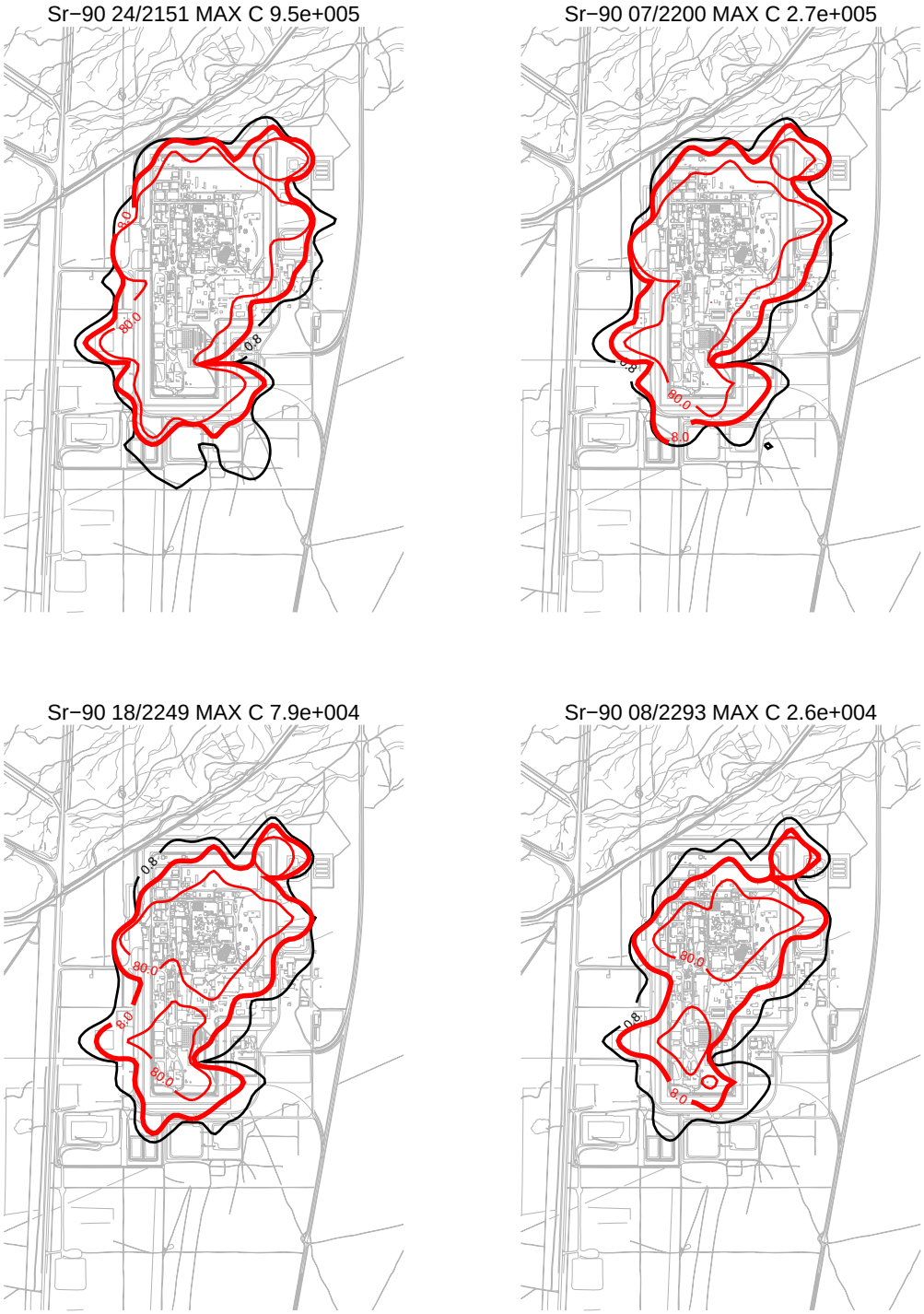

Figure J-11-37. Sr-90 vadose zone concentration stopping anthropogenic water losses in 2035 (horizontal contours) (pCi/L) (MCL = thick red line, 10*MCL = thin red line, MCL/10 = black line).

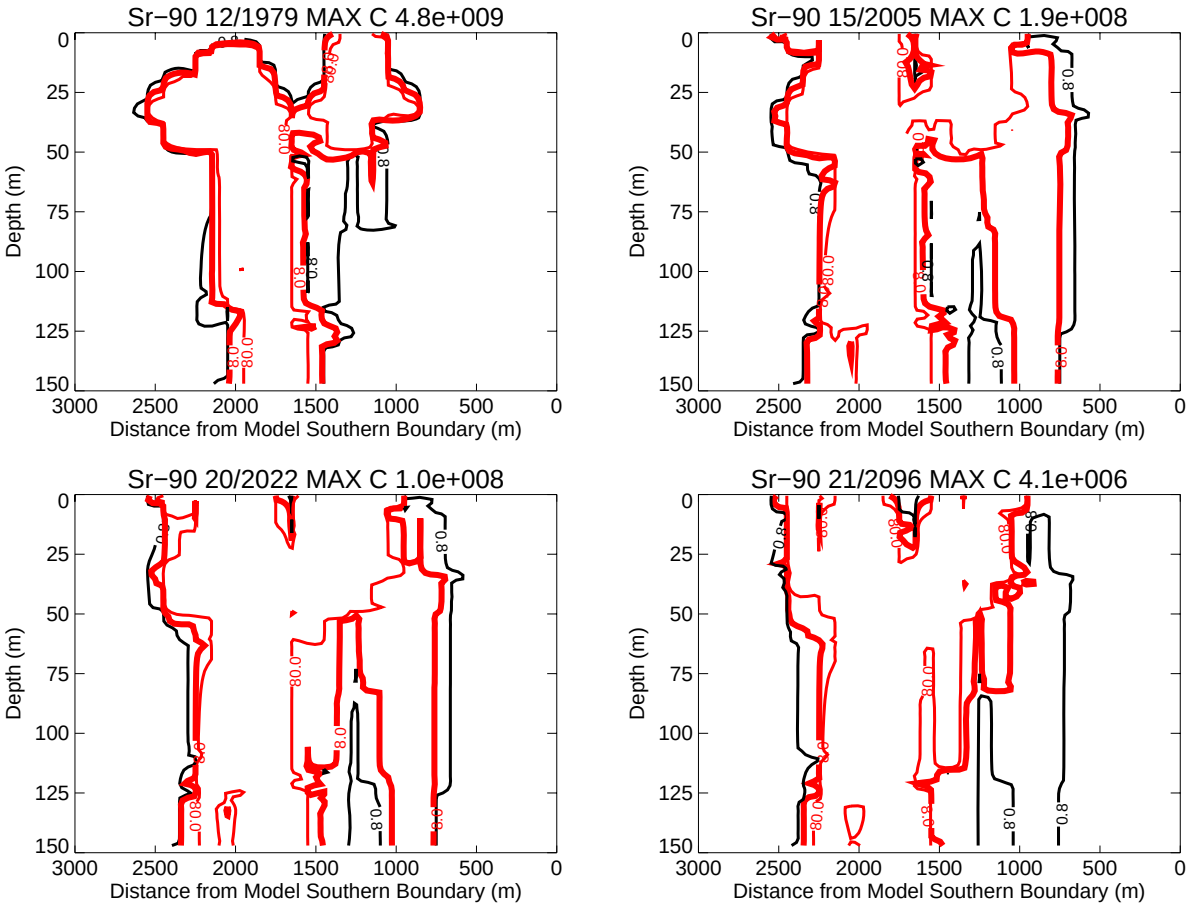

Figure J-11-38. Sr-90 vadose zone concentrations stopping anthropogenic water losses in 2035 (vertical contours) (pCi/L) (MCL = thick red line, 10*MCL = thin red line, MCL/10 = black line).

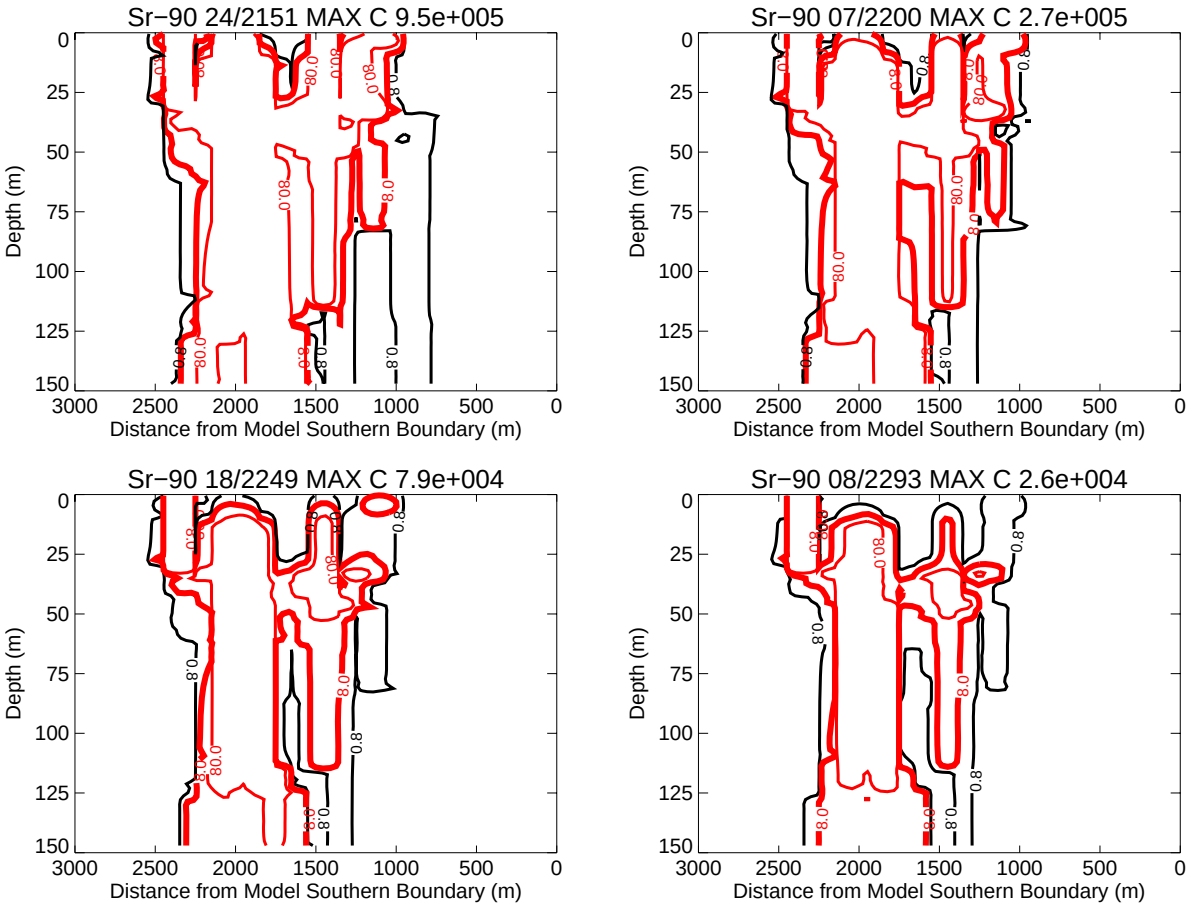

Figure J-11-39. Sr-90 vadose zone concentrations stopping anthropogenic water losses in 2035 (vertical contours) (pCi/L) (continued) (MCL = thick red line, 10*MCL = thin red line, MCL/10 = black line).

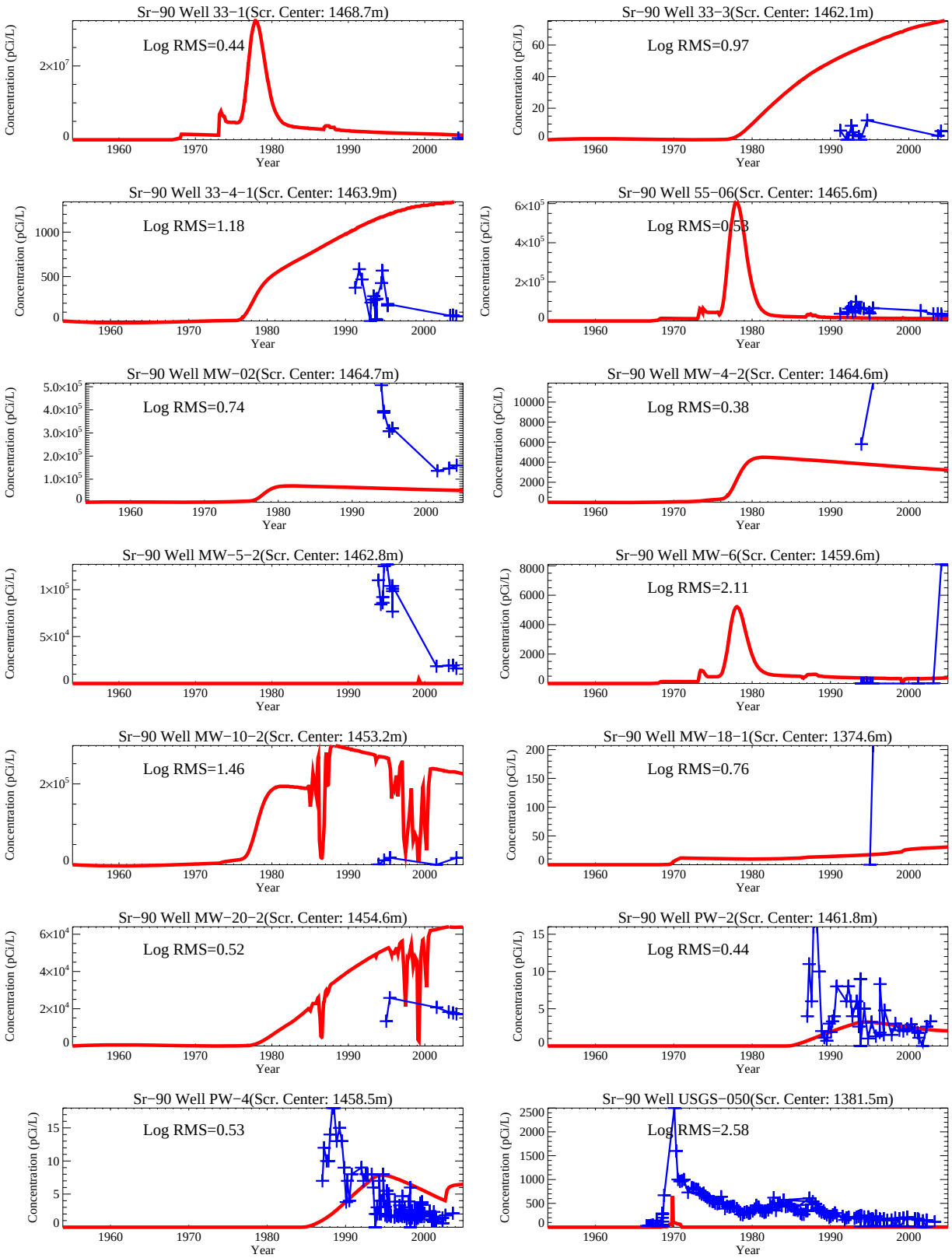

Figure J-11-40. Sr-90 concentration in perched water wells stopping anthropogenic water losses in 2035 (pCi/L) (Measured values = blue crosses, red = model at screen center).

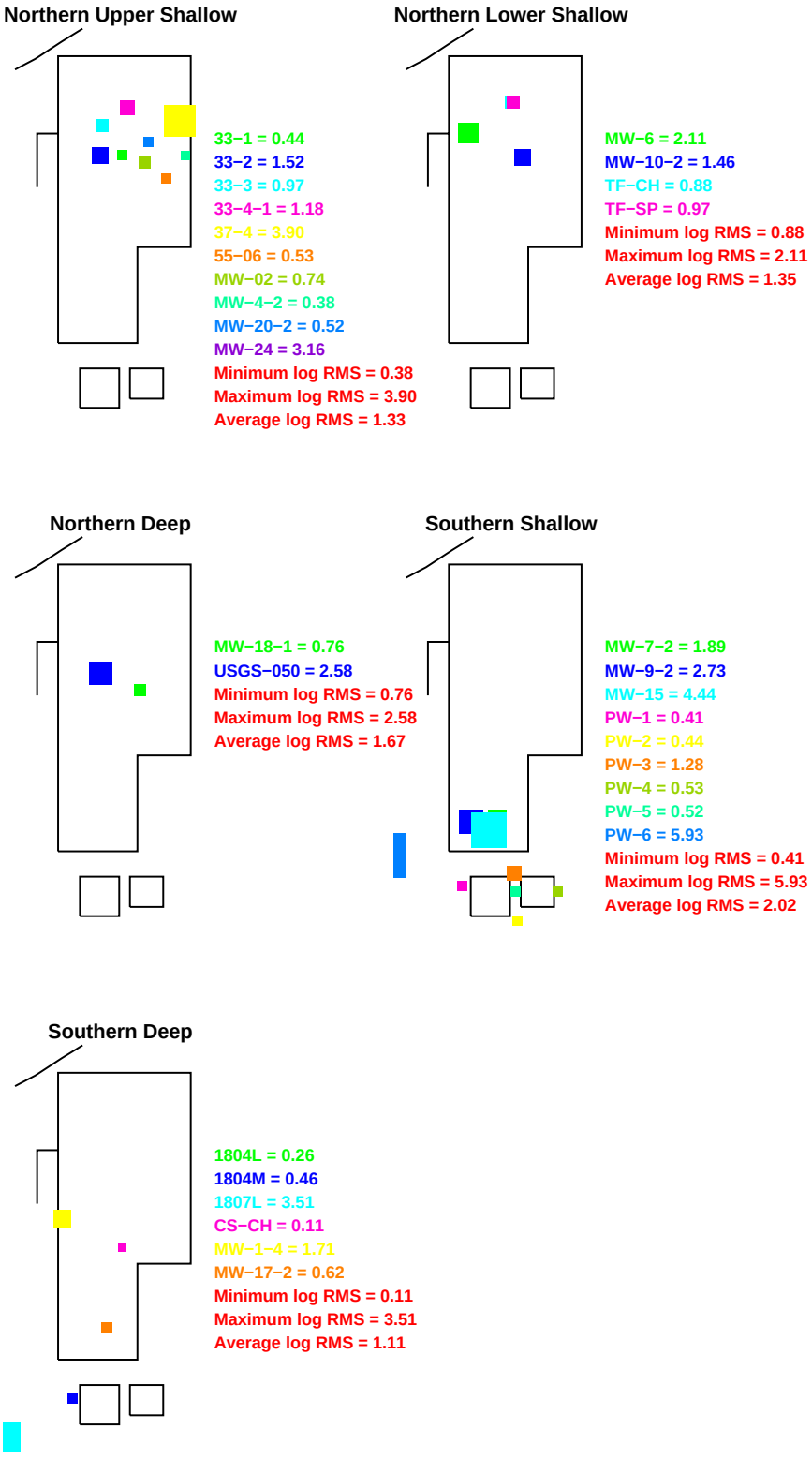

Figure J-11-41. Log 10 Root mean square error (RMS) by depth and northing stopping anthropogenic water losses in 2035.

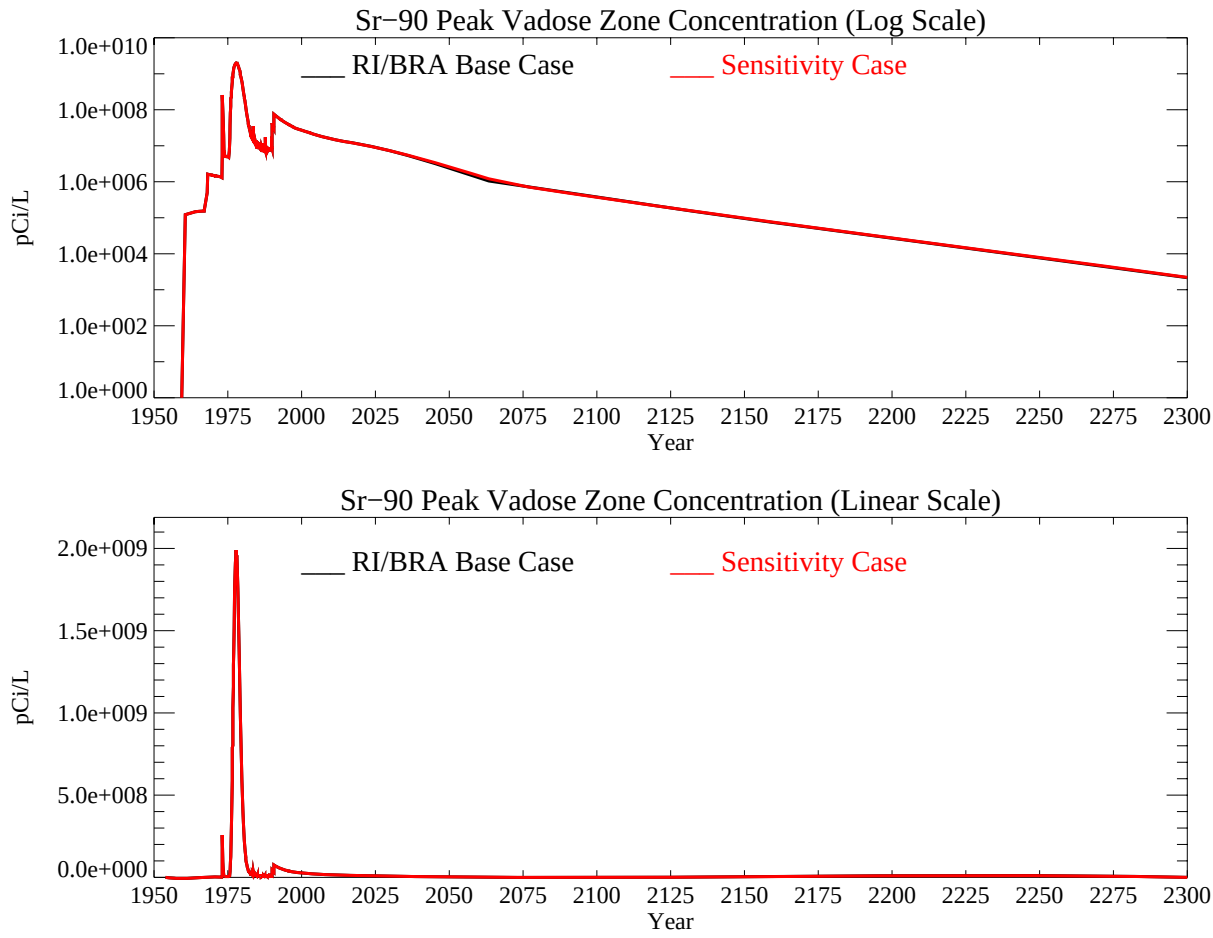

Figure J-11-42. Sr-90 peak vadose zone concentrations stopping anthropogenic water losses in 2035 (pCi/L) with the RI/BRA model in black and this sensitivity run in red.

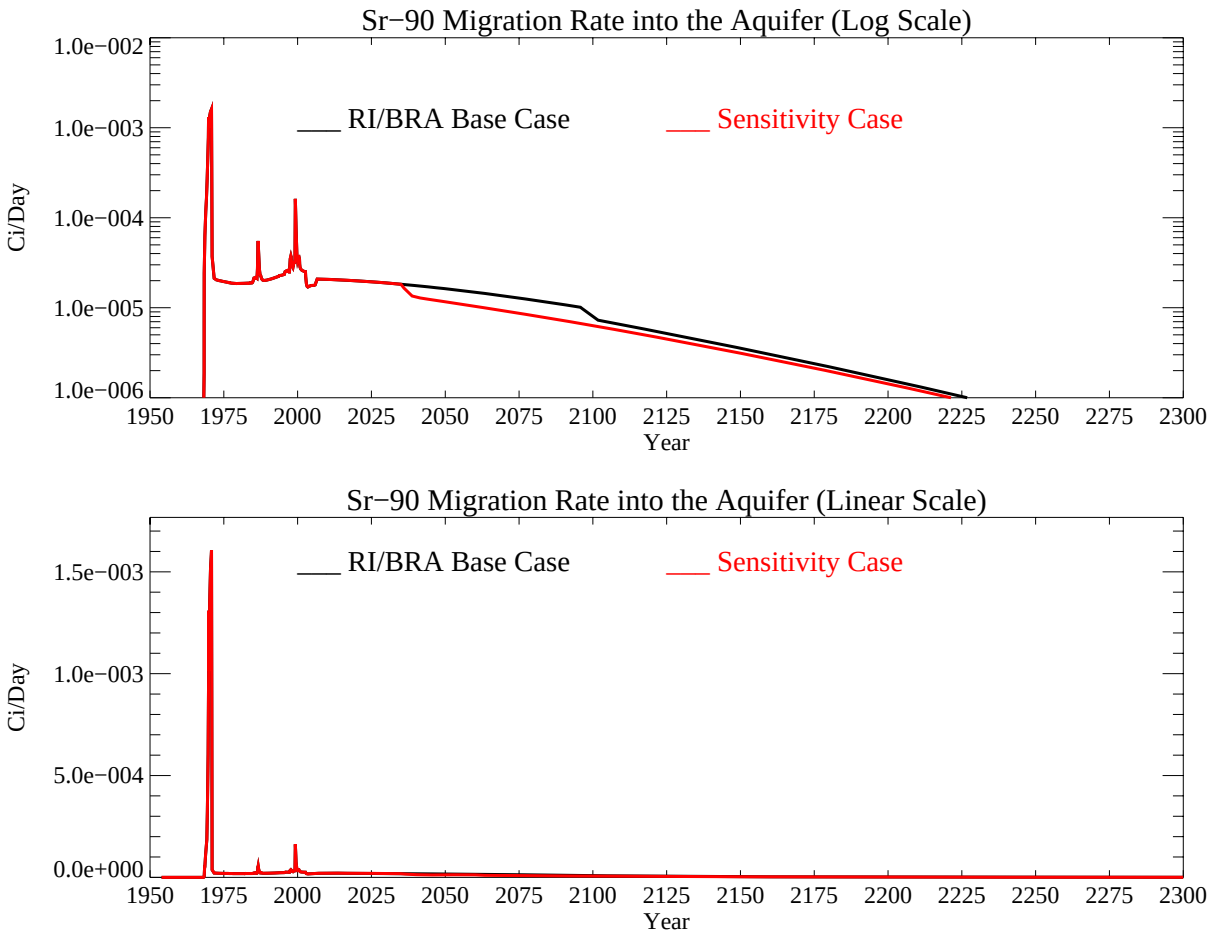

Figure J-11-43. Sr-90 activity flux into the aquifer stopping anthropogenic water losses in 2035 (Ci/day) with the RI/BRA model shown in black, and this sensitivity run in red.

J-11.4.2 Aquifer Sr-90 Simulation Results

The distribution of Sr-90 in the aquifer for the time period spanning 2005-2096 is presented for the far-field in Figure J-11-44 with near-field results given for the 2049-2151 time period in Figure J-11-45. The resultant peak aquifer concentrations are given in Figure J-11-46. Because the Sr-90 originating in the vadose zone does not arrive in the aquifer until the mid 1980's, comparisons to measured data are not presented for aquifer wells.

The peak aquifer Sr-90 concentrations mimic the behavior of the flux out of the vadose zone. As a result, they are identical prior to 2035, and converge back to the RI/BRA predicted concentrations after about year 2125. The simulated Sr-90 concentrations remained above the MCL from 1960 through year 2121, with a predicted peak concentration in year 2095 of 12 pCi/L. This concentration exceeds the MCL by a factor of 1.5. The Sr-90 contour plots presented in Figures J-11-44 and J-11-45 illustrate that although Sr-90 concentrations in the aquifer are predicted to exceed the MCL beyond 2095, the area impacted by Sr-90 above 8 pCi/L is between the tank farm and former percolation ponds in 2096.

The relative insensitivity to early removal of the anthropogenic water was based on the average INTEC water losses of 5 cm/yr. If the anthropogenic water losses are actually focused in northern INTEC, as simulated in Section J-11.3, these results might be quite different.

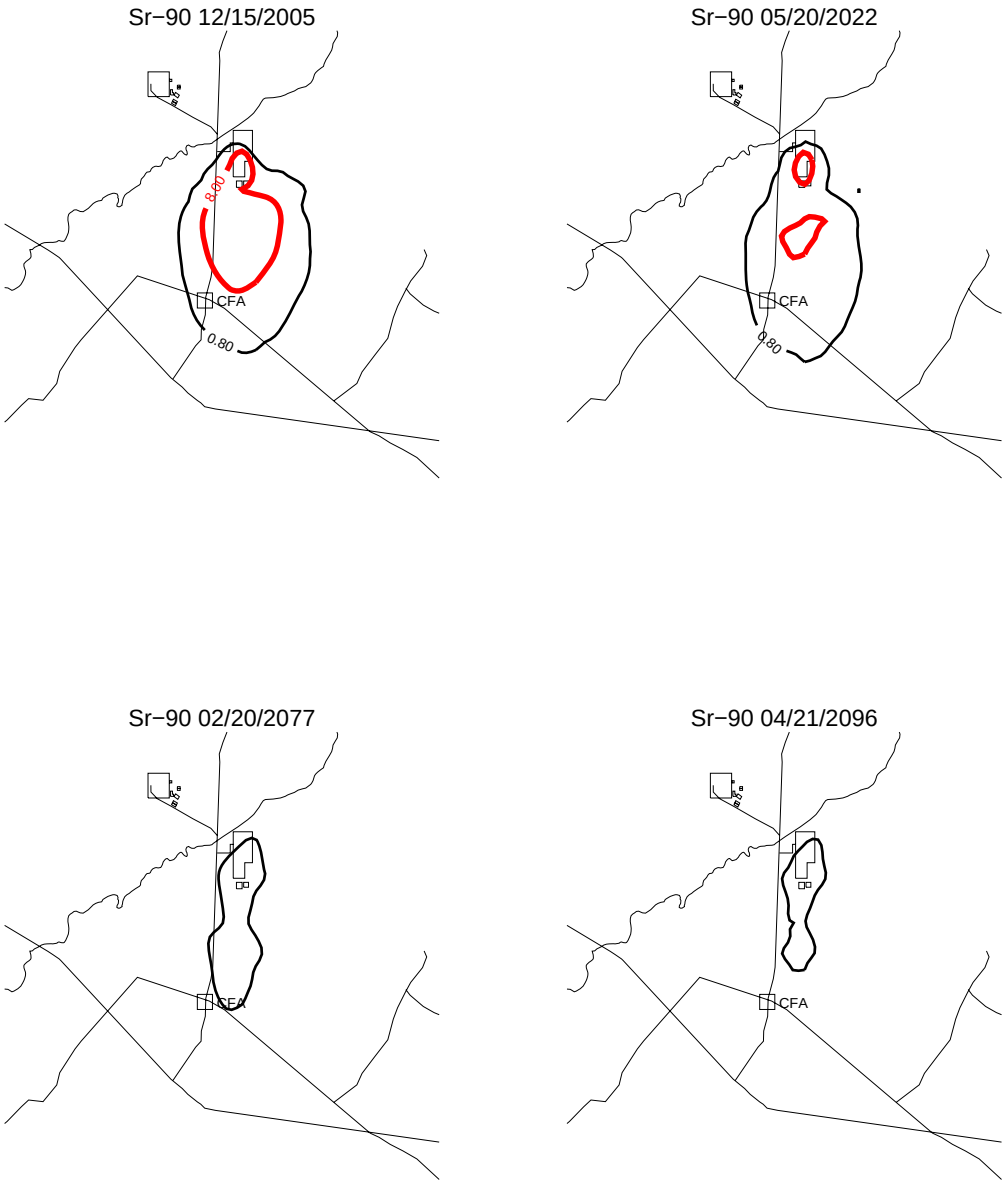

Figure J-11-44. Sr-90 aquifer concentration contours stopping anthropogenic water losses in 2035 (pCi/L) (MCL = thick red line, 10*MCL = thin red line, MCL/10 = black line).

Figure J-11-45. Sr-90 aquifer concentration contours stopping anthropogenic water losses in 2035 (pCi/L) (continued) (MCL = thick red line, 10*MCL = thin red line, MCL/10 = black line).

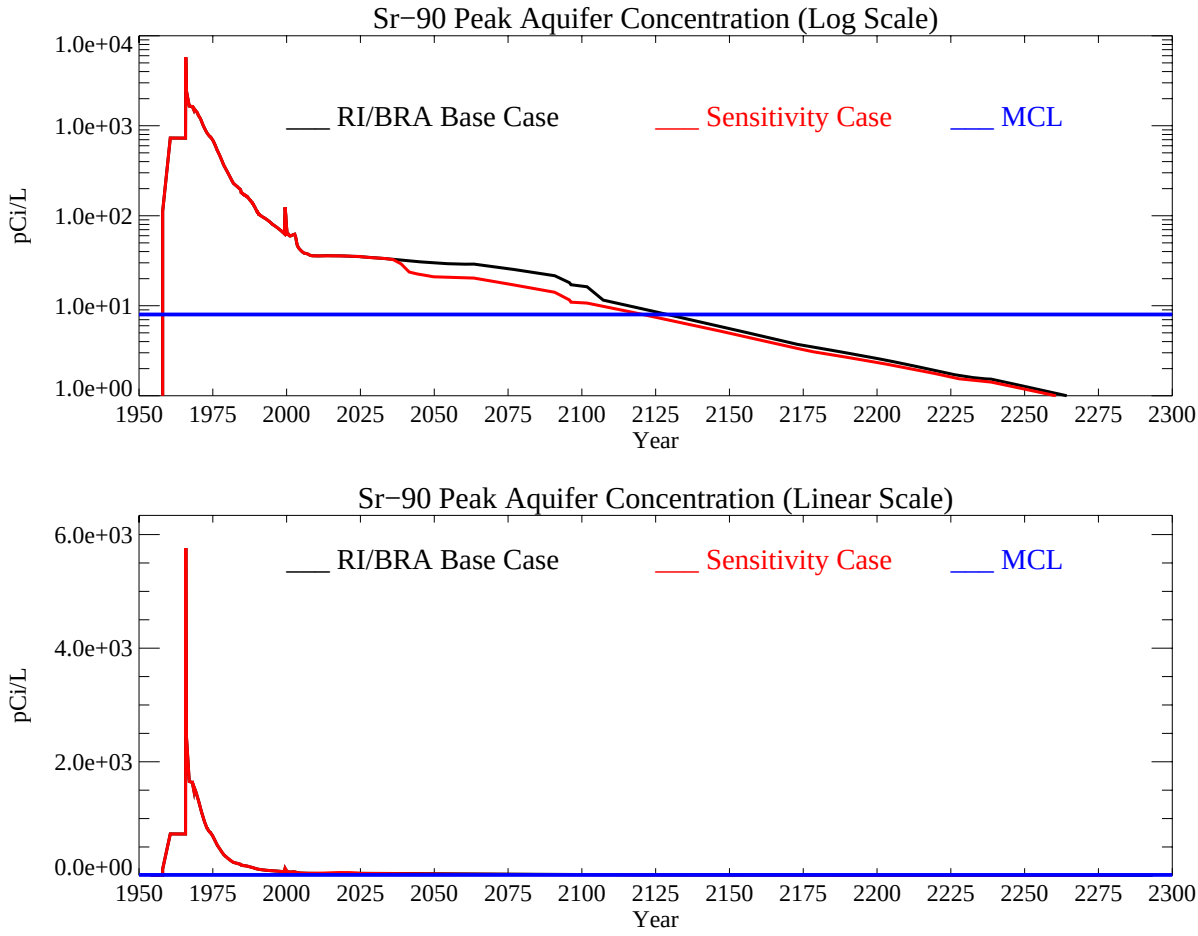

Figure J-11-46. Sr-90 peak aquifer concentrations stopping anthropogenic water losses in 2035 (pCi/L) with the MCL shown in blue, the RI/BRA model in black and this sensitivity run in red.